PREDICTION OF GROUND SUBSIDENCE IN CHIBA PREFECTURE DUE TO LIQUEFACTION BASED ON MACHINE LEARNING

Kazuki Karimai[1], Wen Liu[2] and Yoshihisa Maruyama[3]
[1]Graduate Student, Graduate School of Science and Engineering, Chiba University
1-33 Yayoi-cho, Inage-ku, Chiba-shi, Chiba 263-8522, Japan
Email: 22wm1333@student.gs.chiba-u.jp

[2]Assistant Professor, Graduate School of Engineering, Chiba University
1-33 Yayoi-cho, Inage-ku, Chiba-shi, Chiba 263-8522, Japan
Email: wen.liu@chiba-u.jp

[3]Professor, Graduate School of Engineering, Chiba University
1-33 Yayoi-cho, Inage-ku, Chiba-shi, Chiba 263-8522, Japan
Email: ymaruyam@faculty.chiba-u.jp

KEY WORDS: Machine learning, Liquefaction, Ground subsidence, Regression model

ABSTRACT: The 2011 Great East Japan Earthquake caused severe liquefaction in Urayasu City, Chiba Prefecture, disrupting roads due to sand boiling. Recognizing this threat, Kochi Prefecture performed evacuation drills in anticipation of the Nankai Trough Megathrust Earthquake, revealing challenges like slow evacuation for the elderly and disrupted routes from ground subsidence. To enhance evacuation plans, a broader prediction of ground subsidence is vital, but traditional methods have limitations. This study proposes an improved prediction model using digital national land information, the Japan Engineering Geomorphologic Classification Map (JEGM), and SPT-N values from a nationwide borehole dataset. The model utilizes XGBoost, a machine learning algorithm, enabling rapid computations even for vast datasets. Chiba Prefecture was chosen for analysis due to its previous liquefaction experiences. The model was trained on MESH5 data from the Ministry of Land, Infrastructure, Transport and Tourism. Results showed significant ground subsidence in areas with liquefaction conditions, especially near coasts, rivers, filled lands, and sand dunes due to high ground saturation and sandy soil composition.

1. INSTRUCTIONS

The earthquake that struck off the Pacific coast of the Tohoku region on March 11, 2011, caused large-scale liquefaction in various parts of Japan. This resulted in ground subsidence of roads and sand ejection phenomena leading to raised road surfaces. Such disruptions impeded the passage of emergency vehicles and slowed evacuation speeds. Gabel et al., (2019) pointed out that when evacuation routes experience liquefaction or when the ground undergoes lateral displacement due to lateral flow, it becomes impossible for evacuation vehicles to move and even for evacuees to walk.

Previously, estimates of liquefaction risk commonly used GIS information recorded on a mesh basis for wide-area prediction. However, it's hard to ignore the mechanical properties of the ground, which play a dominant role in liquefaction. By integrating mechanical features with GIS data, there's a potential to enhance the accuracy of predictive models.

In this study, we focus on digital national land information and Japan Engineering Geomorphologic Classification Map (JEGM), and combining them with the N-value obtained from a nationwide borehole dataset, hypothesized that we could learn the trend patterns of ground subsidence and make a broader prediction. Here, we aim to develop a prediction model for ground subsidence to improve liquefaction hazard maps during an earthquake.

2. VERIFICATION AREA AND DATA USED

In this study, a prediction model was constructed using the amount of liquefied land subsidence assumed to be caused by the Nankai Trough giant earthquake as the objective variable. Supervised learning was employed in machine learning to train the prediction model. The dataset for the learning model is compiled on a MESH5 (The width/height of each cell is approximately 250 meters) unit released by the Ministry of Land, Infrastructure, Transport and Tourism in Japan. The training set consists of 1326588 meshes and it is developed using the results discussed by the Nankai Trough Megathrust

Earthquake Model Study Group (Cabinet Office of Japan, 2017), which includes the Tokai Earthquake, the Tonankai and Nankai earthquakes assuming the various scenarios with different locations of hypocentre.

For the ground motion index, the JMA seismic intensity at the baserock (Ia_min_dI) is calculated from the JMA seismic intensity at the surface Ia and the amplification of the JMA seismic intensity between the baserock and the surface dI. Furthermore, the maximum elevation (Max_Elev), minimum elevation (Min_Elev), Relative Relief (Relief), maximum slope angle (Max_Slop_Deg) and minimum slope angle (Min_Slop_Deg) are calculated from the Digital National Land Information (MLIT of Japan, 2020), and the minimum distance from the centre point of the MESH5 to the coastline is calculated as a characteristic quantity related to ground saturation. The shortest distance from the MESH5 centre point to the coastline (Coast_Dist) and the shortest distance to the river (River_Dist) were also added as explanatory variables. The average S-wave velocity (AVS30) of the ground to a depth of 30 m and microtopography classification (JCODE) were added from the dataset developed by Wakamatsu et al., (2013). The Height Above Nearest Drainage (HAND) was added as a parameter indicating height from the channel (Yamazaki et al., 2018; Rennó et al., 2008).

The SPT-N value, which is an indicator of the strength of the ground, is downloaded from the Kunijiban national ground information search site (MLIT of Japan et al., 2020). Specifically, SPT-N values were added as explanatory variables for every 1 m from the ground surface to a depth of 10 m. However, as the depth at which SPT-N values are obtained is not always an integer value, data interpolation is carried out in accordance with the input layer. For the depth-N map obtained by the interpolation process, the nearest borehole points from the target mesh are assigned to each 1 m from the ground surface (B1, B2, B3, B4, B5, B6, B7, B8, B9 and B10). The shortest distance from the center point of MESH5 to the boring point was added as an explanatory variable as (B_Dist). These data were aggregated to MESH5 units.

3. MACHINE LARNING MODEL

In this study, we construct a prediction model by sequentially combining weak learners based on gradient boosting using XGBoost (eXtreme Gradient Boosting). During the model's learning process, the connected weak learners operate to minimize the overall loss of the model. This involves repeatedly adjusting weights at each stage to reduce the difference between predicted and actual values, thereby explicitly fitting the relationship between explanatory variables and target variables. Through this process, the model engages in feature extraction from the explanatory variables and learns the trend patterns of the data, enabling it to predict and explain from a new dataset. Notably, XGBoost proactively generates interactive feature variables from the product of explanatory variables, allowing for the consideration of causality among multiple variables. As such, it can represent interactions in high dimensions when multiple features are combined, leading us to anticipate the construction of a robust regression prediction model.

4. RESULTS AND DISSCATION

4.1 Factor analysis based on SHAP

Using the trained model, we calculated the SHAP values (Lundberg and Lee, 2017). Figure 1 shows the contribution (SHAP feature importance) of each explanatory variable in the ground subsidence prediction model. It should be noted that the relative contributions of each variable do not necessarily relate to the magnitude of ground subsidence. Contribution scores are metrics to assess the extent to which various factors influence a particular phenomenon or result. According to Figure 1, the most influential variable on ground subsidence was the base seismic intensity (Ia_min_dI). This can be attributed to the fact that the rate of increase in pore water pressure within the ground changes with the magnitude of the base seismic intensity, hence its high contribution to ground subsidence. The average S-wave velocity up to a depth of 30m (AVS30) and the lowest elevation (Min_Elev) also had significant contributions. Variables related to ground amplification and topographic information ranked high.

These results are considered geotechnically reasonable since these variables are dominant factors for liquefaction. Although the contribution of borehole data is small per variable, the cumulative contribution of each group is higher than other variables. This suggests that it's effective to include borehole data as explanatory variables in the liquefaction-induced ground subsidence prediction model. Geotechnically, the SPT-N value is an indicator of ground hardness. By combining this with features related to topography and seismic motion, an improvement in the predictive model's expressiveness is anticipated.

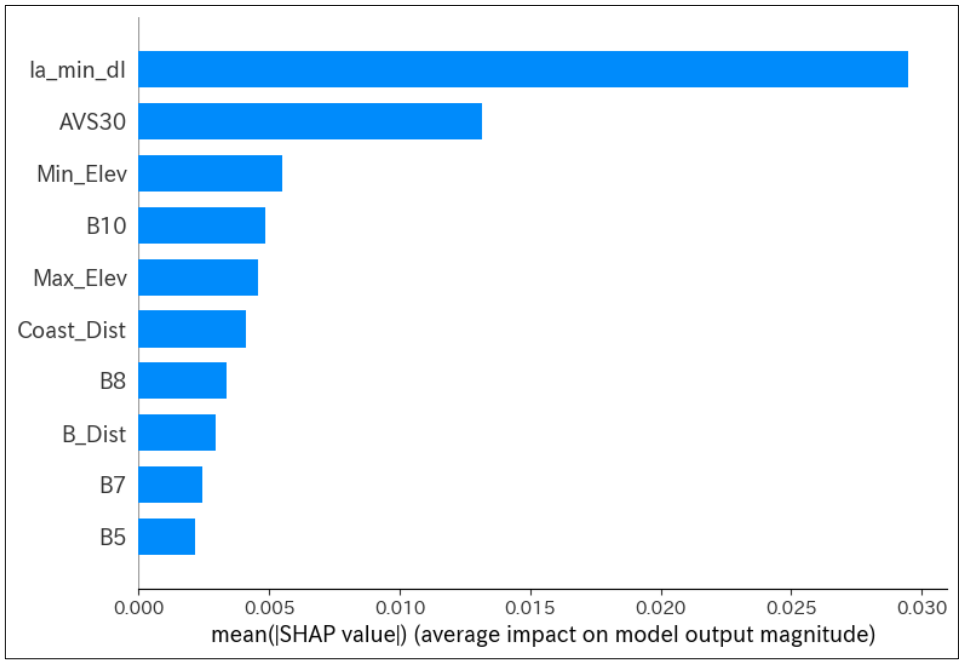

Figure 1. Feature importance of each feature in the prediction model

4.2 Ground subsidence map of Chiba Prefecture

The prediction of ground subsidence was conducted using the trained model. Figures 2 and 3 show the predicted ground subsidence maps for the entire Chiba Prefecture when subjected to seismic intensity on the engineering bedrock of 5.5 (JMA seismic intensity: 6-) and 5.0 (JMA seismic intensity: 5+), respectively. According to the results, it can be inferred that areas comprising reclaimed land and sandy layers experienced an approximate subsidence of 0.06 meters, whereas

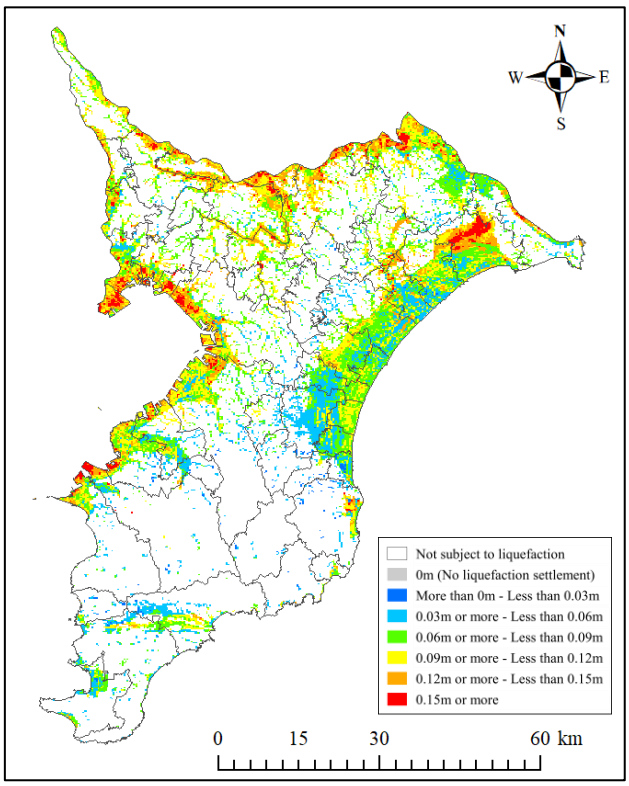

Figure 2. Seismic intensity on the engineering bedrock (JMA seismic intensity: 6-)

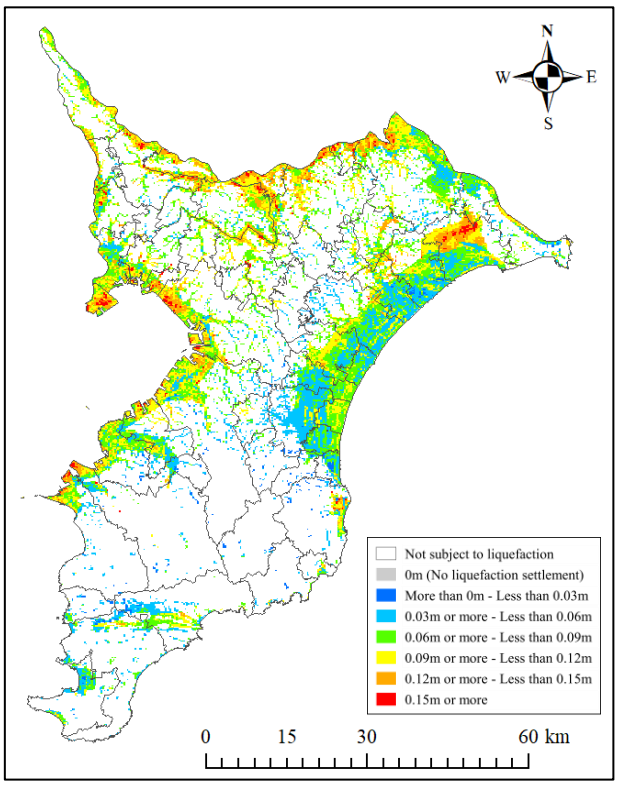

Figure 3. Seismic intensity on the engineering bedrock (JMA seismic intensity: 5+)

areas closer to water bodies exhibited subsidence of more than 0.12 meters. Significant subsidence was observed in areas with a high proportion of sand, such as reclaimed lands, coastal regions, and the areas surrounding the Tone River and Inbanuma.

This indicates the prominent manifestation of ground subsidence in areas susceptible to liquefaction, suggesting that the predictions align geotechnically. The prediction model seems to have effectively extracted features from the training set. Traditional liquefaction hazard maps only provided binary classifications indicating whether liquefaction would occur or not. However, by explicitly and quantitatively showing the amount of ground subsidence as in Figures 2 and 3, it becomes possible to anticipate realistic scenarios, taking into account the reduced evacuation speed and potential blockages in evacuation routes after an earthquake.

5. CONCLUSION

In this study, we aimed to enhance liquefaction hazard mapping. A prediction model for ground subsidence due to liquefaction was developed utilizing machine learning, integrating the Digital National Land Information, microtopography classification, and ground motion intensity. Using this model, we generated maps representing expected ground subsidence for different seismic intensity levels in Chiba Prefecture. The contribution of each explanatory variable was rigorously assessed using SHAP values. Variables that were heavily influenced by the factors leading to liquefaction showed significant contributions, suggesting that the outcomes are geotechnically reasonable. Furthermore, the inclusion of grouped borehole data as explanatory variables notably improved the model's predictive capability. In future studies, we intend to incorporate additional geotechnical information, such as density, grain size, and consistency, to further improve the prediction model's accuracy.

6. REFERENCES

Cabinet Office of Japan, 2017. Nankai Trough Megathrust Earthquake Model Study Group, https://www.bousai.go.jp/jishin/nankai/model/, Accessed 10 Sep 2023 (in Japanese).

Gabel, L. L. S., O'Brien, F. E., Bauer, J. M. and Allan, J. C., 2019. Tsunami evacuation analysis of communities surrounding the Coos Bay estuary: Building community resilience on the Oregon coast. Tech. Rep. O-19-07, Oregon Department of Geology and Mineral Industries, p. 65.

Lundberg, S. M., and Lee, S. I., 2017. A Unified Approach to Interpreting Model Predictions. Adv. Neural Inf. Process. Syst. 30, pp. 4765-4774. DOI: https://arxiv.org/abs/1705.07874.

MLIT of Japan, 2023. Digital National Land Information Download Site, http://nlftp.mlit.go.jp/ksj/, Accessed 10 Sep 2023 (in Japanese).

MLIT of Japan, PWRI of Japan, PARI of Japan, 2020. National ground information search site, http://www.kunijiban.pwri.go.jp, Accessed 10 Sep 2023 (in Japanese).

Rennó, C. D., Nobre, A. D., Cuartas, L. A., Soares, J. V., Hodnett, M. G., Tomasella, J. and Waterloo, M. J., 2008. HAND, a new terrain descriptor using SRTM-DEM: Mapping terra-firme rainforest environments in Amazonia. Remote Sensing of Environment, 112(9), pp. 3469-3481, DOI: https://doi.org/10.1016/j.rse.2008.03.018.

Wakamatsu, K., and Matsuoka, M., 2013. Nationwide 7.5-arc-second Japan engineering geomorphologic classification map and Vs30 zoning. J. Disaster Res, 8(5), pp. 904-911, DOI: https://doi.org/10.20965/jdr.2013.p0904.

Yamazaki, D., Togashi, S., Takeshima, A., and Sayama, T., 2018. High-resolution flow direction map of Japan. J Jpn Soc Civil Eng (B1), 74(5), pp. I_163-I_168, DOI: https://doi.org/10.2208/jscejhe.74.5_I_163 (In Japanese).